Efficient Defect Healing in Catalytic Carbon Nanotube Growth

Qinghong Yuan,[1,2] Zhiping Xu,[3] Boris I. Yakobson,[4] and Feng Ding[1,2,4,*]

[1]National Laboratory of Infrared Physics, Shanghai Institute for Technical Physics, Chinese Academy of Sciences, Yu Tian Road 500, Shanghai 200083, Peoples Republic of China,
[2]Institute of Textiles and Clothing, Hong Kong Polytechnic University, Kowloon, Hong Kong, Peoples Republic of China
[3]Department of Engineering Mechanics, Tsinghua University, Beijing 100084, Peoples Republic of China
[4]Department of Mechanical Engineering and Materials Science, Rice University, Houston, TX 77005, USA

(Received 6 February 2012; published 15 June 2012)

The energetics of topological defects (TDs) in carbon nanotubes (CNTs) and their kinetic healing during the catalytic growth are explored theoretically. Our study indicates that, with the assistance of a metal catalyst, TDs formed during the addition of C atoms can be efficiently healed at the CNT-catalyst interface. Theoretically, a TD-free CNT wall with 10^8–10^{11} carbon atoms is achievable, and, as a consequence, the growth of perfect CNTs up to 0.1–100 cm long is possible since the linear density of a CNT is ~100 carbon atoms per nanometer. In addition, the calculation shows that, among catalysts most often used, Fe has the highest efficiency for defect healing.

DOI: 10.1103/PhysRevLett.108.245505 PACS numbers: 61.48.De, 31.15.A−, 81.16.Hc

A perfect single-walled carbon nanotube (SWCNT) has a well-defined atomic structure, which is depicted by a pair of chiral indexes, (n, m). Tubes with same (n, m) have an identical wall structure and can be either metallic (if $n - m = 3i$, where i is an integer) or semiconducting (if $n - m = 3i + 1$ or $3i + 2$) [1]. Therefore, high quality SWCNTs with the same chiral indexes (n, m) are highly desired for many applications, e.g., high performance sensors and field effect transistors.

Experimentally synthesized SWCNT has a two dimensional (2D) cylindrical wall of a honeycomb lattice, in which any non-six-membered ring (6MR), e.g., a pentagon, a heptagon, or an octagon, should be considered as a topological defect (TD). A capped SWCNT can be viewed as an elongated fullerene and the numbers of different types of polygons in it follow

$$\Sigma n_p(6 - p) = 12, \tag{1}$$

where n_p is the number of p-membered rings (pMRs) [2]. Considering only 5, 6, 7, and 8 MRs, Eq. (1) can be rewritten as $n_5 - n_7 - 2n_8 = 12$. Neglecting the 12 pentagons on both caps of a SWCNT, the numbers of pMRs in a SWCNT wall satisfy

$$n_5 - n_7 - 2n_8 = 0. \tag{2}$$

Equation (2) indicates that an isolated non-6MRs cannot appear in a SWCNT wall alone. As illustrated in Figs. 1(a) and 1(b), an isolated pentagon turns a SWCNT into a sharp cone and a heptagon turns a SWCNT into a horn. In other words, TDs in a SWCNT wall must appear in the form of non-6MR clusters. Among all the potential forms of non-6MR clusters, the pentagon-heptagon pair (5|7) is the simplest one as it contains only two non-6MRs. Other forms include the 5|7/7|5 for the Stone-Wales defect [3], 7|5/5|7 for ad-dimer [4,5], 5|8|5 for di-vacancy [6], and contain at least 3 non-6MRs. Both previous studies and our present calculations demonstrated that 5|7 has the lowest formation energy among them [3–7] and, therefore, 5|7 is also the most possible form of TD in SWCNT walls.

It is important to note that a 5|7 is an edge dislocation core in a SWCNT wall that changes the tube's chirality [8,9]. As shown in Figs. 1(c) and 1(d), two 5|7 pairs with different orientations change a (10,0) SWCNT into (9,0) and (9,1), respectively. Because 5|7 is the most possible TD cluster, we conclude that a SWCNT with a single

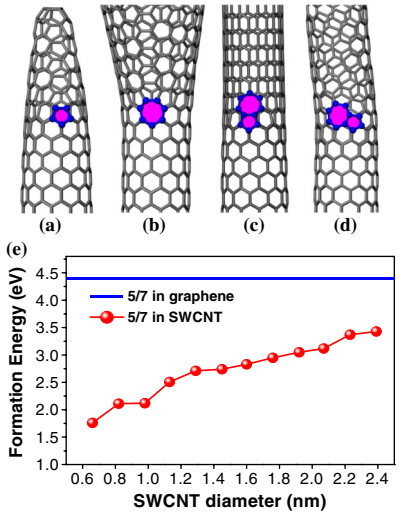

FIG. 1 (color online). An isolated pentagon turns a (10,0) SWCNT into a cone shape (a) and a heptagon turns it into a horn (b). A 5|7 that, along the direction of the tube axis, changes the chirality of the tube to (9,0) (c) and a 5|7 with different orientation changes the tube into a (9,1) one (d). (e) The formation energies of a 5|7 in SWCNTs vs the tube diameter (red real line with circles) and in graphene (blue real line) (see the supplemental Material for details of the calculation [26].

chirality along its whole wall is mostly free of any topological defects.

At the atomic level, during the growth of a SWCNT, every polygon in a tube wall is formed at the CNT-catalyst interface by the addition of C atoms. As is well documented, the incorporation of two C atoms is required to form a hexagon and the addition of a C monomer or trimer leads to the formation of a pentagon or heptagon [10,11]. Considering that the C monomer, dimer, and trimer have very similar formation energies on mostly used catalyst surfaces, Fe, Co, and Ni [12–15], the formation of non-6MRs during C insertion is inevitable. Thus, an efficient healing of TDs is required for the growth of high quality SWCNTs.

Experimentally, SWCNTs or few-walled CNTs up to 20 cm have been synthesized [16–18]. Signs that these CNTs have consistent chiral indexes along the wall have been observed. For example, 18 cm long SWCNTs were found to have uniform electronic properties along the whole stem [16]. In a recent report, the electron diffraction patterns clearly revealed that a 3.5 cm long CNT stem preserves exactly same chiral indexes [17]. To maintain such a perfect CNT, in which about 10^{10} polygons existed in its wall, an extremely high efficiency of defect healing that leads to a defect concentration less than 10^{-10} is required.

In this Letter, the energetic stability and the kinetic healing of TDs during catalytic SWCNT growth are studied by using the density functional theory calculations. Our study indicates that, with the assistance of the catalyst, most TDs (pentagons, heptagons, and 5|7 pairs) can be healed efficiently. At an optimum condition, the concentration of TDs can be reduced to 10^{-8}–10^{-11} and, as a consequence, the growth of a 0.1–100 cm long perfect SWCNT is theoretically possible.

Firstly, let us consider the energetic requirement of growing a macroscopically perfect crystal. Under the condition of thermodynamic equilibrium, the number of defects, N_d, in a crystal is

$$N_d = N_s \exp\left(-\frac{E_f}{k_b T}\right), \tag{3}$$

where N_s is the number of lattice sites in the crystal, k_b is the Boltzmann constant, E_f is the formation energy of the defect, and T is the temperature. A 10 cm long SWCNT has $\sim 10^{10}$ polygons in its wall; thus, to maintain its perfection, the number of defects must be no greater than 1 or $N_d/N_s = \exp[-E_f/(k_b \times T)] < 10^{-10}$. Under the typical CNT growth condition, $T \sim 800$–$100\,^{\circ}\mathrm{C}$ or $k_b T \sim 0.08$–0.1 eV, so we have

$$E_f > -(k_b \times T)\ln(10^{-10}) \sim 2.0 \text{ eV}. \tag{4}$$

Equation (4) is the thermodynamic requirement for the growth of macroscopically long perfect SWCNTs. As shown in Fig. 1(e), the E_f of the most energetically preferred TD unit, 5|7, in a CNT wall, fulfill Eq. (4) for $D > 1.0$ nm, where D is the tube diameter. Furthermore, the E_f of 5|7 can be as high as 4.4 eV in the graphene due to the absence of curvature energy.

Next, let us turn to the kinetics of defect healing during SWCNT growth. As well stated in the literature, the growing CNT has an open end attached to a stepped edge on a catalyst particle surface and the armchair (AC) sites are active for carbon insertion [19–21]. As shown in Figs. 2(a) and 2(b), an AC graphene edge attached to a stepped metal surface was adopted to model a fraction of the SWCNT-stepped catalyst interface. Such a model has been verified in previous studies of CNT growth [19,22]. The generalized gradient approximation with the Perdew-Burke-Ernzerhof functional [23] was used in all calculations. The barriers of defect healing are calculated by the climbing nudged energy band method incorporated in the Vienna *ab initio* software package (VASP) [24,25] (see Supplemental Material for details of the modeling and methods of calculation [26]).

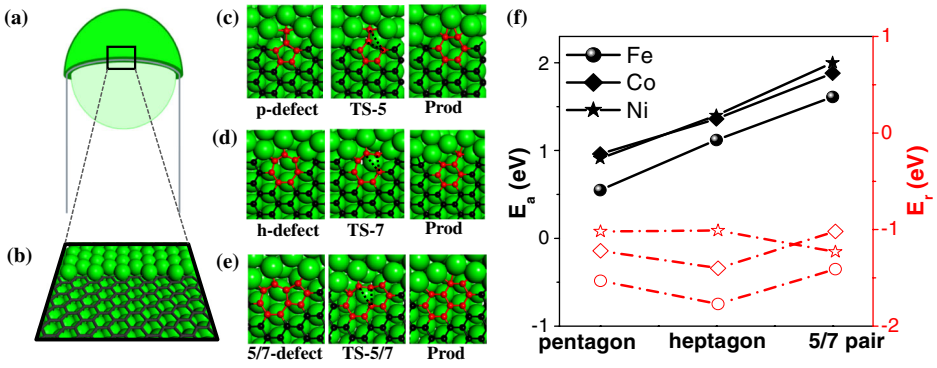

FIG. 2 (color online). (a) The SWCNT-catalyst particle interface, where a circular tube's open end is attached to a step edge on the catalyst particle. (b) A fraction of the SWCNT-catalyst step [a step along the (211) direction on the (111) surface of the fcc crystal] interface is modeled as an interface of the graphene-stepped metal surface. (c)–(e) The healing of the pentagon (**p** defect), heptagon (**h** defect), and pentagon-heptagon pair (5|7) and the corresponding geometries (original defect formations, transition states and products after healing) involved. (f) The energy barrier (E^*) (black real line with symbols) and the reaction energy (E_r) (red dashed line with symbols) for the **p**, **h**, and 5|7 defects healing on stepped Fe(111)/Co(111)/Ni(111) surfaces.

As shown in Figs. 2(c)–2(e), the healing of three typical defects, pentagons (**p**), heptagons (**h**), and their pair (5|7) are considered. As a **p** cannot be healed by itself, we considered the formation of a pentagon with a dangling C atom as the initial structure [Fig. 2(c)]. The healing of the **p** defect can be achieved by breaking a C-C bond and reforming another one [Fig. 2(c)]. The healing of the **h** defect leads to the formation of a new hexagon with a dangling C atom [Fig. 2(d)]. The 5|7 can be transformed into a pair of hexagons (6|6) by rotating a shoulder C-C bond on one side of the heptagon. Among them, as discussed before, the **p** and **h** can be frequently formed during the addition of C atoms into the growing end of a CNT. Thus, during the growth of high quality SWCNTs, the healing of **p** or **h** must be very efficient. As shown in Fig. 2(f), the barriers of **p** and **h** healing, E^*, are 0.55/0.96/0.91 and 1.12/1.36/1.40 eV on three typical catalysts, Fe/Co/Ni, respectively. Considering the typical SWCNT growth temperature, $T \sim 800\,^\circ$–$1000\,^\circ$C or $k_bT \sim 0.1$ eV, both **p** and **h** can be healed in a very short period of $\tau \sim 10^{-13} \times \exp(E^*/k_bT)$ s $= 10^{-8} - 10^{-7}$ s. So, fast defect healing allows the fast growth of high quality SWCNTs.

Despite of the very fast healing of **p** and **h**, some of them can survive at a small probability. As the Euler's rule does not allow the existence of individual **p** or **h** in a SWCNT wall, those **p** or **h** that survived must be transformed into a non-6MR cluster form. Here we only consider the most possible formation, 5|7, which can be formed by the addition of a **h**(**p**) near a survived **p**(**h**). As shown in Fig. 2(e), a 5|7 pair on the edge of a SWCNT can be transformed into two hexagons (i.e., 5|7 → 6|6) by rotating a C-C bond. The calculated barriers of the "5|7 → 6|6" reaction on Fe/Co/Ni surfaces are 1.61/1.88/2.00 eV, respectively, demonstrating that the healing of 5|7 defects is more difficult than the healing of isolated **p** or **h**.

Figure 2(f) represents the comparison of the energy barrier, E^*, and reaction energy, E_r, for the healing of the three aforementioned defects on Fe, Co, and Ni surfaces. Comparing with Co and Ni, defect healing on the Fe surface has the lowest E^*, and E_r. This result indicates that Fe is the best catalyst for the growth of high quality SWCNTs. This is in agreement with the experimental fact that Fe is the catalyst used the most for high quality SWCNT synthesis [18,19,27,28]. Thus, considering the very expensive calculations, only catalyst Fe is considered hereafter.

The above calculations revealed a high defect healing efficiency on the outmost edge of a SWCNT. During SWCNT growth, a 5|7 moves gradually into the tube wall if it is not healed on the outmost edge. In order to calculate the number of survived TDs in the SWCNT wall, the healing of 5|7 pairs during its motion from the outmost front to the SWCNT wall must be considered. As shown in Fig. 3 (details can be found in the Supplemental Material [26]), the healing of the 5|7 at different distances from the growing front can be achieved via very similar processes, namely, "5|7 → 6|6." It can be seen that the barrier becomes higher and higher and the reactive energy becomes lower and lower when the 5|7 moves toward the SWCNT wall (Fig. 3). When a 5|7 is totally embedded into the hexagonal network (the 5|7-4 in Fig. 3), the barrier raises sharply to 3.22 eV, which means the healing of the 5|7 pairs inside the SWCNT wall during growth is nearly impossible. Simultaneously, the reaction energy decreases from −1.5 eV, on the front, to −2.5 eV in the wall, which exceeds the formation energy requirement, Eq. (4).

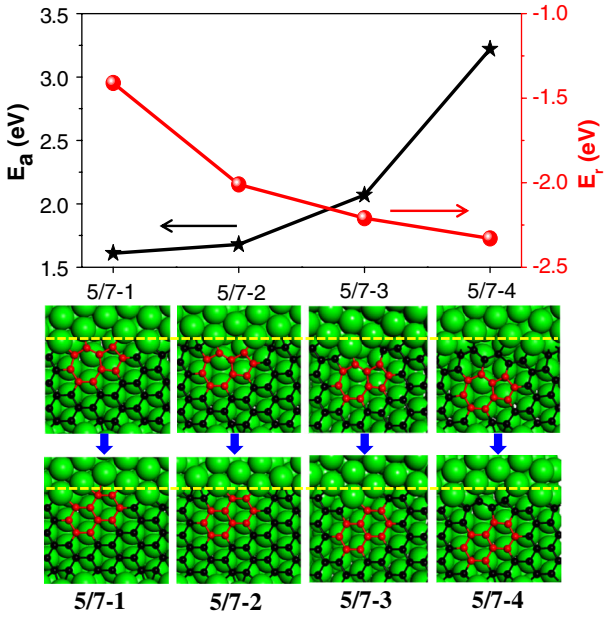

FIG. 3 (color online). The 5|7 defect healing during its motion from the tube edge to the wall and the corresponding energy barriers (E^*) (black line with stars) and reaction energies (E_r) (red line with circles). Among the four steps, the 5|7 disappears in 5|7-1, -2, -3, but 5|7-4 leads to a glide of the 5|7 to the front. (For details of the defect healing process, see Ref. [26].) Fe was considered as the catalyst in this study.

With all these barriers and reaction energies, the calculation of the TD concentration in the SWCNTs grown under a specific growth condition (e.g., temperature and growth rate) is possible. As can be seen in Fig. 3, the healing of defects occurs at different depths from the front-most edge and thus the concentration of 5|7 is a function of the distance from the growing front. The time scale of the defect evolution at each depth is determined by the growth rate of the CNT, $\tau = \Delta h/R$, where $\Delta h \sim 0.1$ nm is the distance between two neighboring steps and R is the CNT growth rate.

For the defect healing at each step, the concentration evolution follows

$$dC = -CK_+dt + (1 - C)K_-dt, \tag{5}$$

where C is the concentration of the defect, $K_+ = (k_bT/h) \times \exp(-E^*/k_bT)$ and $K_- = (k_bT/h)\exp[-(E^* + E_r)/k_bT]$ are the reaction constants of the reaction and the reverse process (i.e., 6|6 → 5|7) whose barrier is $E^* + E_r$. The solution of Eq. (5) is

$$C = C_e + C' \times \exp(-(k_bT/h) \times \{\exp(-E_r/k_bT) + \exp[-(E_r + E^*)/k_bT]\} \times t), \tag{6}$$

where $C_e = [1 + \exp(E_r/k_bT)]^{-1}$ is the defect concentration at thermal equilibrium ($t \to \infty$). $C' = C_0 - C_e$, in which C_0 is the defect concentration at $t = 0$.

For defects healing at the front-most (5|7–1), two types of defects, **p** and **h**, are considered and the survived **p** and **h** should be transformed into the form of 5|7 and moved to the tube wall. The initial concentrations of **p** and **h**, $C(\mathbf{p})_0$ and $C(\mathbf{h})_0$, depend on the atomic details of carbon atom addition. Here we set both $C(\mathbf{p})_0$ and $C(\mathbf{h})_0$ to be 10%, which is in agreement with the molecular dynamic simulated CNT formation [28,29]. It will be seen that, because of the low barriers of defect healing, the effect of $C(\mathbf{p})_0$ and $C(\mathbf{h})_0$ on the tube quality is negligible at most tube growth temperatures ($T > 1000$ K).

Figure 4(a) shows the concentration of the pentagon $[C(\mathbf{p})_1]$ and heptagon $[C(\mathbf{h})_1]$ as functions of the temperature at the growth rate of $R = 100$ μm/s or $\tau = 1.0$ μs. It can be seen that the healing of **p** is very efficient and $C(\mathbf{p})_1$ is reduced to 10^{-15} at $T = 500$ K. When $T > 500$ K, the reverse processes become considerable and thus the $C(\mathbf{p})_1$ goes higher and higher and reaches $\sim 10^{-8}$ at $T = 1000$ K. Because of the relatively high barrier of **h** healing, the optimum healing that occurs is 930 K. As we discussed before, neither the **p** nor **h** defect can exist in a CNT wall alone so they must be turned into 5|7 when they go deeper from the front-most edge. Thus, we consider their summation, $C(5/7)_1 = C(\mathbf{p})_1 + C(\mathbf{h})_1$, as the initial concentration of 5|7 for the healing of $i = 2$.

The concentrations of 5|7 at different depths vs temperatures are shown in Fig. 4(b). The local minimum of the curves at $T = 930$ K corresponds to the effective healing of both **p** and **h** on the front-most edge. The local minimum at $T = 1280$ K in the curves of $C(5|7)_2$, $C(5|7)_3$, and $C(5|7)_4$ corresponds to the efficient 5|7 healing at the stage of $i = 2$, whose barrier is the second lowest (Fig. 3). The inflection point at $T = 1500$ K corresponds to the healing of defect at the stage of $i = 3$, whose barrier is 2.1 eV. It can be clearly seen that the curves of $C(5|7)_3$ and $C(5|7)_4$ are nearly identical, indicating that there is no further defect healing if the 5|7 was surrounded with hexagons. Therefore, $C(5|7)_4$ can be regarded as the concentration of 5|7 in the tube wall, $C(5|7)_w = C(5|7)_4$.

The $C(5|7)_w$ vs temperature with SWCNT growth rates from 10^{-2} to 10^2 μm/s are shown in Fig. 4(c). It is clear that, at any temperature, the defect concentration of a fast growing SWCNT is always higher than that of a slow growing one and all curves resemble a similar shape. So, the defects can be healed more efficiently at a lower growth rate. At the growth rate of $R = 1$ μm/s, which is a very fast experimental SWCNT growth rate [18], the CNT defect concentration may reach 10^{-9} at an optimum temperature of $\sim$800 or $\sim$1100 K. It should be noted that the density functional theory calculations might underestimate the activation barrier up to 0.5 eV [30,31]. At the temperature of the CNT growth, $k_bT \sim 0.1$ eV, such an error may slow down the defect healing rate by a factor of $\sim \exp(-0.5\text{eV}/k_bT) \sim 10^{-2}$. However, in a realistic condition of SWCNT growth, in which numerous hydrogen, oxygen, or water molecules are involved, both the barriers and the reaction energies of defect healing can be greatly reduced. As shown in [26], the involving of a H atom or an OH group reduces the barriers and reaction energies approximately 60% and 20%, respectively. Beyond that, the quality of a SWCNT can be further improved by low temperature growth with a slow growth rate.

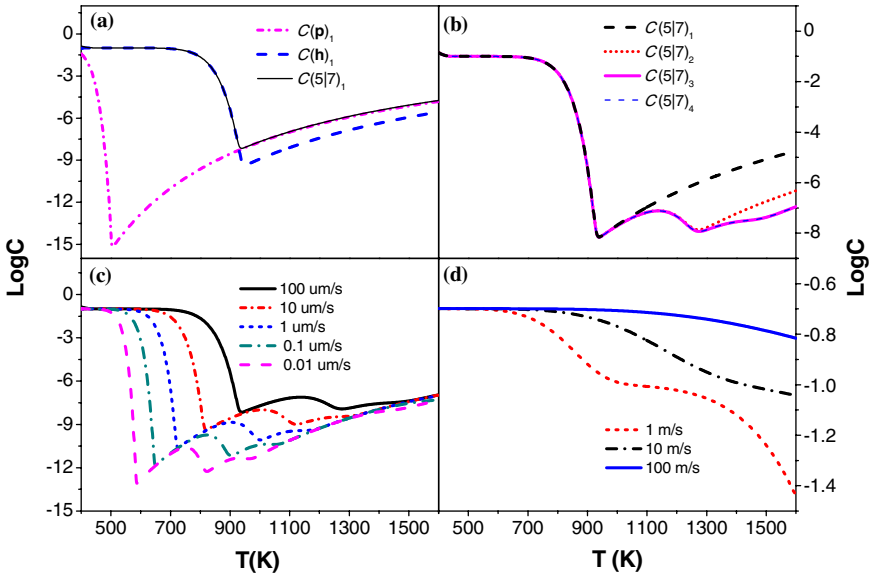

FIG. 4 (color online). (a) The concentrations of pentagon $[C(\mathbf{p})_1]$, heptagon $[C(\mathbf{h})_1]$, and their summation $[C(5|7)_1]$ on the front-most edge of a growing SWCNT as functions of temperature (T) at the growth rate of 100 μm/s; (b) The concentrations of $C(5|7)_i$ vs T at different depths from tube edge at the growth rate of 100 μm/s; (c) Concentrations of survived 5|7 in the CNT wall, $C(5|7)_w$ vs T at different growth rates; (d) Concentrations of survived 5|7 in the CNT wall at very fast growth rates. Fe was considered as the catalyst in this study.

For example, the growth of SWCNT at 700 K with the rate of 1 μm/s leads a SWCNT quality of 10^{-11}, which indicates that it is theoretically possible to grow meter long SWCNTs with a perfect wall.

Figure 4(d) shows the 5|7 concentration vs T at three very fast growth rates, 1, 10, and 100 nm/ns, which correspond to the SWCNT growth in classical [32–35] tight-binding [29] and *ab initio* [36] molecular dynamic simulations. It can be clearly seen that the defect healing rarely occurs at these growth rates: only 10%, 40%, and 60% of defects formed during the addition of C atoms are healed. So, we can conclude that the limited simulation time is responsible for the very defective SWCNT formation observed in various molecular dynamic simulations [29,32–36].

In conclusion, we systematically explored the concentration of the most likely formed topological defects, pentagons-heptagons pairs (5|7 pairs), in the SWCNT wall. Our calculations demonstrated that the limit of 5|7 concentration can be as low as 10^{-8}–10^{-11} and the growth of macroscopic long SWCNTs is theoretically possible. The study also shows that, relative to Co and Ni, Fe is the best catalyst for defect healing.

The work at Rice University was initially supported by the National Science Foundation and at later stages by the Office of Naval Research Grant No. N00014-11-1077. The work at Shanghai Institute for Technical Physics was supported in part by the National Natural Science Foundation of China Grants (No. 61006090, No. 10990104, and No. 60976092). The work at Tsinghua University was supported by NSFC through Grant No. 11002079.

*tcfding@inet.polyu.edu.hk

[1] T. W. Odom, J. L. Huang, P. Kim, and C. M. Lieber, Nature (London) **391**, 62 (1998).
[2] F. Ding, Y. Lin, P. O. Krasnov, and B. I. Yakobson, J. Chem. Phys. **127**, 164703 (2007).
[3] E. Ertekin, D. C. Chrzan, and M. S. Daw, Phys. Rev. B **79**, 155421 (2009).
[4] D. Orlikowski, M. Buongiorno Nardelli, J. Bernholc, and C. Roland, Phys. Rev. Lett. **83**, 4132 (1999).
[5] M. Sternberg, L. A. Curtiss, D. M. Gruen, G. Kedziora, D. A. Horner, P. C. Redfern, and P. Zapol, Phys. Rev. Lett. **96**, 075506 (2006).
[6] J. Kotakoski, A. V. Krasheninnikov, and K. Nordlund, Phys. Rev. B **74**, 245420 (2006).
[7] The formation energy of the 5/7 defect is between 1.5 and 3.5 eV, depending on the tube diameter, while the formation energies of other forms of defects are ~4.5 eV for SW 5|7/7|5 (Ref. [2]), 4 ~ 6 eV for 7|5/5|7 (Refs. [3,4]), and 4 ~ 8 eV for 5|8|5.
[8] B. I. Yakobson, Appl. Phys. Lett. **72**, 918 (1998).
[9] E. C. Neyts, A. C. T. van Duin, and A. Bogaerts, J. Am. Chem. Soc. **133**, 17225 (2011).
[10] M. S. Dresselhaus, G. Dresselhaus, and P. Avouris, *Carbon Nanotubes: Synthesis, Structure, Properties and Applications* (Springer-Verlag, Berlin, 2001).
[11] H. Chen, W. G. Zhu, and Z. Y. Zhang, ACS Nano **4**, 6665 (2010).
[12] H. Chen, W. G. Zhu, and Z. Y. Zhang, Phys. Rev. Lett. **104**, 186101 (2010).
[13] J. F. Gao, Q. H. Yuan, H. Hu, J. J. Zhao, and F. Ding, J. Am. Chem. Soc. **133**, 5009 (2011).
[14] X. S. Wang, Q. Q. Li, J. Xie, Z. Jin, J. Y. Wang, Y. Li, K. L. Jiang, and S. S. Fan, J. Phys. Chem. C **115**, 17695 (2011).
[15] The formation energy of monomer, dimer, and trimer on Fe/Co/Ni surfaces is −1.75, −0.90, −0.38/0.66, 0.57, 0.74/0.89, 0.72, 0.84 eV, respectively.
[16] X. S. Wang, Q. Q. Li, J. Xie, Z. Jin, J. Y. Wang, Y. Li, K. L. Jiang, and S. S. Fan, Nano Lett. **9**, 3137 (2009).
[17] Q. Wen, W. Z. Qian, J. Q. Nie, A. Y. Cao, G. Q. Ning, Y. Wang, L. Hu, Q. Zhang, J. Q. Huang, and F. Wei, Adv. Mater. **22**, 1867 (2010).
[18] Q. Wen, R. F. Zhang, W. Z. Qian, Y. R. Wang, P. H. Tan, J. Q. Nie, and F. Wei, Chem. Mater. **22**, 1294 (2010).
[19] F. Ding, A. R. Harutyunyan, and B. I. Yakobson, Proc. Natl. Acad. Sci. U.S.A. **106**, 2506 (2009).
[20] F. Abild-Pedersen, J. K. Nørskov, J. R. Rostrup-Nielsen, J. Sehested, and S. Helveg, Phys. Rev. B **73**, 115419 (2006).
[21] S. Helveg, C. López-Cartes, J. Sehested, P. L. Hansen, B. S. Clausen, J. R. Rostrup-Nielsen, F. Abild-Pedersen, and J. K. Nørskov, Nature (London) **427**, 426 (2004).
[22] Q. H. Yuan, H. Hu, and F. Ding, Phys. Rev. Lett. **107**, 156101 (2011).
[23] J. P. Perdew, K. Burke, and M. Ernzerhof, Phys. Rev. Lett. **77**, 3865 (1996).
[24] G. Kresse and J. Furthmüller, Phys. Rev. B **54**, 11169 (1996).
[25] G. Kresse and J. Furthmuller, Comput. Mater. Sci. **6**, 15 (1996).
[26] See Supplemental Material at http://link.aps.org/supplemental/10.1103/PhysRevLett.108.245505 for details of the modeling and methods of calculation.
[27] L. X. Zheng, M. J. O'Connell, S. K. Doorn, X. Z. Liao, Y. H. Zhao, E. A. Akhadov, M. A. Hoffbauer, B. J. Roop, Q. X. Jia, and R. C. Dye *et al.*, Nature Mater. **3**, 673 (2004).
[28] S. J. Kang, C. Kocabas, T. Ozel, M. Shim, N. Pimparkar, M. A. Alam, S. V. Rotkin, and J. A. Rogers, Nature Nanotech. **2**, 230 (2007).
[29] A. J. Page, Y. Ohta, S. Irle, and K. Morokuma, Acc. Chem. Res. **43**, 1375 (2010).
[30] K. P. Jensen, B. O. Roos, and U. Ryde, J. Chem. Phys. **126**, 014103 (2007).
[31] W. Koch and M. C. Holthausen, in *A Chemist's Guide to Density Functional Theory* (Wiley-VCH, Weinheim, 2001), p. 300.
[32] M. A. Ribas *et al.*, J. Chem. Phys. **131**, 224501 (2009).
[33] F. Ding, K. Bolton, and A. Rosen, J. Phys. Chem. B **108**, 17369 (2004).
[34] J. Zhao, A. Martinez-Limia, and P. B. Balbuena, Nanotechnology **16**, S575 (2005).
[35] H. Amara, C. Bichara, and F. Ducastelle, Phys. Rev. Lett. **100**, 056105 (2008).
[36] J. Y. Raty, F. Gygi, and G. Galli, Phys. Rev. Lett. **95**, 096103 (2005).